
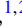
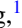
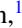




Suppressing reactivity in a degenerate Fermi molecular gas via the statistical potential

Yan-Peng Bai ¹, Jing-Lun Li ^{1,2}, Gao-Ren Wang ^{1,*}, Zhong-Bo Chen ¹, Bo-Wen Si ¹ and Shu-Lin Cong ^{1,†}

¹*School of Physics, Dalian University of Technology, Dalian 116024, China*

²*Institut für Quantenmaterie and Center for Integrated Quantum Science and Technology (IQST), Universität Ulm, 89069 Ulm, Germany*

 (Received 26 November 2021; revised 14 March 2022; accepted 11 April 2022; published 21 April 2022)

We present a simple theoretical model used for describing the suppressing reactivity of an ultracold Fermi molecular gas in a degenerate regime via the statistical potential. The statistical potential originates from the symmetry properties of the wave function of identical particles, and is derived by using the density matrix. We use our theoretical model to well reproduce recent experimental results of a potassium-rubidium molecule gas in the deep quantum degenerate regime reported by De Marco *et al.* [*Science* **363**, 853 (2019)]. The suppression of the chemical reaction rate observed in the experiment is quantitatively reproduced by using the p -wave scattering volume as an adjusting parameter. The strength of spatial correlation can be intuitively captured by the statistical potential.

DOI: [10.1103/PhysRevA.105.043314](https://doi.org/10.1103/PhysRevA.105.043314)

I. INTRODUCTION

The achievement of quantum degeneracy [1–7] in ultracold gases provides an ideal platform to study many-body phenomena and chemical reactions in molecular physics. Though the quantum degeneracy in a trapped Fermi atomic gas has been observed 20 years ago [4], the preparation of a degenerate molecular gas in the ground state has been one of the most challenging goals due to the complex internal degree of freedom of the molecules [8–10].

Recently, De Marco *et al.* reported the creation of an ultracold potassium-rubidium molecule gas in the deep quantum degenerate regime [10]. A significant suppression of the reaction rate was observed below 0.6 times the Fermi temperature, and the Bethe-Wigner threshold law no longer works [10,11]. In order to explain this suppression, one has to go beyond the pure two-body loss model to include additional mechanisms, such as the statistical behavior of the molecular gas, etc. [12–14]. In the degenerate regime, the de Broglie wavelength of a particle is comparable to or greater than the interparticle spacing, so there is a strong spatial correlation between the particles even in an ideal gas. For Fermi gases, the collision between particles has to overcome the effective repulsive potential according to the Pauli exclusion principle. This repulsive potential is generally called the statistical potential, and its formula can be derived by comparing the spatial probability density of particles in quantum mechanics with that in classical mechanics [15]. This work aims to study the effect of the statistical behavior of a Fermi molecular gas on the reaction rate in a degenerate regime. To understand and interpret the experimental observations, we introduce the

statistical potential in the two-body scattering. We find that the suppression of the reaction rate can be well reproduced.

II. THE STATISTICAL POTENTIAL OF A NONIDEAL FERMI GAS

The radial Schrödinger equation for two-body scattering is written as

$$\left(-\frac{d^2}{dr^2} + \frac{L(L+1)}{r^2} + V_{\text{eff}}\right)\psi(r) = E\psi(r), \quad (1)$$

where L is the relative orbital angular momentum. r and E are the scaled radius and collision energy, respectively. The length scale is defined as $\beta_\alpha = (2\mu C_\alpha/\hbar^2)^{1/(\alpha-2)}$ with $\mu = m/2$ being the reduced mass [16]. C_α is the dispersion coefficient, and $\alpha > 2$ is the exponent of the model potential $-C_\alpha/r^\alpha$. The energy scale is $s_E = \hbar^2/(2\mu\beta_\alpha^2)$. The effective potential, $V_{\text{eff}} = V(r) + V_{\text{sta}}(r)$, contains the interparticle interaction $V(r)$ and the statistical potential $V_{\text{sta}}(r)$ originating from the symmetry properties of the wave function of identical particles [15].

The statistical potential is obtained by using the density matrix. The diagonal element of the density matrix $\hat{\rho}_0$ of an ideal gas ensemble in the coordinate representation is given by

$$\begin{aligned} &\langle r_1, \dots, r_N | \hat{\rho}_0 | r_1, \dots, r_N \rangle \\ &= \frac{\langle r_1, \dots, r_N | e^{-\beta\hat{H}_0} | r_1, \dots, r_N \rangle}{Z_N^0(\mathcal{V}, \beta)}, \end{aligned} \quad (2)$$

where r_i is the coordinate of the i th particle, and \hat{H}_0 is the total Hamiltonian of N free particles. Equation (2) represents the probability density, where the particles in gas are located at r_1, \dots, r_N . The partition function for the ideal gas is given by

$$Z_N^0(\mathcal{V}, \beta) = \int d^{3N}r \langle r_1, \dots, r_N | e^{-\beta\hat{H}_0} | r_1, \dots, r_N \rangle, \quad (3)$$

*gaoren.wang@dlut.edu.cn

†shlcong@dlut.edu.cn

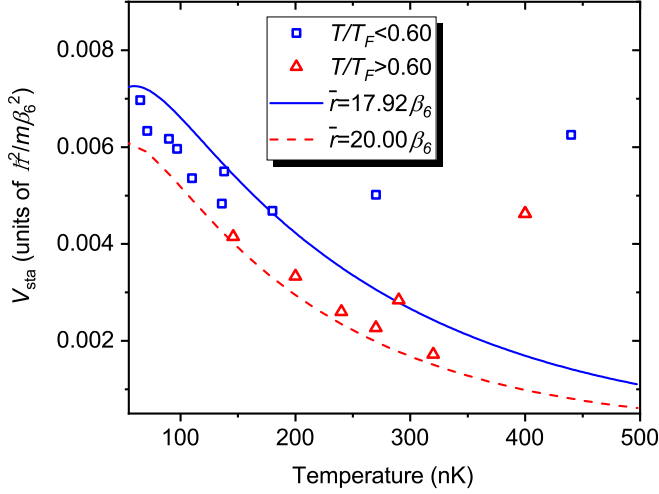


FIG. 1. The statistical potential V_{sta} as a function of temperature T for the average interparticle spacing $\bar{r} = 17.92\beta_6$ (solid line) and $20.00\beta_6$ (dashed line). The magnitudes of statistical potential calculated from the experimental data at different Fermi temperatures (squares and triangles) [10] (see Table I). Squares and triangles correspond to $T/T_F < 0.60$ and > 0.60 , respectively. The p -wave scattering volume a_1 is taken to be $-12.97a_0^3$.

where $d^{3N}r = dr_1 \cdots dr_N$, \mathcal{V} is the volume of gas, and $\beta = 1/k_B T$ with k_B being the Boltzmann constant. The classical version of Eq. (2) is expressed as

$$\int \rho_0 d^{3N}p = \frac{1}{N!h^{3N}} \frac{1}{Z_N^c} \int e^{-\beta\mathcal{H}} d^{3N}p, \quad (4)$$

where $Z_N^c = 1/(N!h^{3N}) \int e^{-\beta\mathcal{H}} d^{3N}r d^{3N}p$ is the classical partition function, $d^{3N}p = dp_1 \cdots dp_N$, and \mathcal{H} is the classical Hamiltonian. In order to obtain the same result as Eq. (2) from Eq. (4), a statistical potential needs to be added to the classical Hamiltonian \mathcal{H} . For an ideal Fermi gas, the statistical potential V_{sta}^0 is expressed as [15]

$$V_{\text{sta}}^0 = -\frac{1}{\beta} \ln[\mathcal{V}^N \langle r_1, \dots, r_N | \hat{\rho}_0 | r_1, \dots, r_N \rangle]. \quad (5)$$

However, the hypothesis of an ideal gas is insufficient to deal with the decay of molecular gas in the quantum degenerate regime. When the interaction between particles is included, the statistical potential for the Fermi gas in the interacting regime is given by

$$V_{\text{sta}} = -\frac{1}{\beta} \ln[\mathcal{V}^N \langle 1, \dots, N | \hat{\rho} | 1, \dots, N \rangle], \quad (6)$$

with

$$\langle 1, \dots, N | \hat{\rho} | 1, \dots, N \rangle = \frac{\langle 1, \dots, N | e^{-\beta\hat{H}} | 1, \dots, N \rangle}{Z_N(\mathcal{V}, \beta)}, \quad (7)$$

where \hat{H} is the Hamiltonian of the nonideal gas. r_1, \dots, r_N in Eq. (5) is replaced by $1, \dots, N$ in Eq. (6) in order to distinguish from the wave function of the ideal gas. The partition function for a nonideal gas is given by

$$Z_N(\mathcal{V}, \beta) = \sum_{\{m_l\}} \prod_{l=1}^N \frac{1}{m_l!} \left(\frac{\mathcal{V}}{\lambda^3} b_l \right)^{m_l}, \quad (8)$$

where b_l is the l -cluster integral, namely,

$$b_l(\mathcal{V}, \beta) = \frac{1}{l! \lambda^{3l-3} \mathcal{V}} \int d^3r_1 d^3r_2 \cdots d^3r_l U_l(1, 2, \dots, l), \quad (9)$$

where $U_l(1, 2, \dots, l)$ is the cluster function [15]. $\{m_l\}$ is a set of integers that satisfies the condition $\sum_{l=1}^N l m_l = N$. In the following, we take $N = 2$ as an example. For the ideal Fermi gas, $\langle r_1, r_2 | e^{-\beta\hat{H}_0} | r_1, r_2 \rangle = [1 - \exp(-2\pi r^2/\lambda^2)]/(2\lambda^6)$ and Eq. (5) is reduced to $V_{\text{sta}}^{0(2)}(r) = -k_B T \ln[1 - \exp(-2\pi r^2/\lambda^2)]$ [15], where $\lambda = \hbar(2\pi\beta/m)^{1/2}$ is the average thermal wavelength with mass m . For the Fermi gas in the interacting regime, $\langle 1, 2 | \hat{\rho} | 1, 2 \rangle = \langle 1, 2 | e^{-\beta\hat{H}} | 1, 2 \rangle / Z_2(\mathcal{V}, \beta)$ with $Z_2(\mathcal{V}, \beta) = 1/2(\mathcal{V}/\lambda^3)^2 + \mathcal{V}b_2/\lambda^3$. Then the statistical potential of a nonideal Fermi gas is given by

$$V_{\text{sta}}^{(2)}(r) = -k_B T \ln \frac{2\lambda^6 \langle 1, 2 | e^{-\beta\hat{H}} | 1, 2 \rangle}{1 + 2b_2\lambda^3/\mathcal{V}} \\ \approx -k_B T \ln \frac{1 - e^{-2\pi r^2/\lambda^2}}{1 + 2b_2\lambda^3/\mathcal{V}}. \quad (10)$$

In the asymptotic region of $r \gg 1$, the potential $V(r) \rightarrow 0$, and $\langle 1, 2 | e^{-\beta\hat{H}} | 1, 2 \rangle$ can be approximatively replaced by $\langle r_1, r_2 | e^{-\beta\hat{H}_0} | r_1, r_2 \rangle$ in Eq. (10). The 2-cluster integral b_2 can be expressed in terms of a two-body scattering phase shift as

$$b_2 = 2^{-5/2} + 2^{3/2} \frac{\lambda^2}{\pi^2} \sum_{L=\text{odd}} (2L+1) \int_0^\infty dk k \eta_L(k) e^{-\beta\hbar^2 k^2/m}, \quad (11)$$

where η_L is the energy-dependent partial phase shift [15]. For the Fermi gas, the reaction rate is given by

$$K = \frac{g}{k} \sum_{L=\text{odd}} (2L+1)(1 - |S_L|^2), \quad (12)$$

where S_L is the S matrix for the L -partial wave. For the universal case, the S matrix is expressed as $S_L = (-1)^{L+1} r^{oi}$, where r^{oi} is the quantum reflection coefficient induced by the long-range potential [16]. The quantum reflection coefficient r^{oi} can be obtained by solving Eq. (1) [16,17]. $g = 1$ for distinguishable particles and $g = 2$ for identical particles in the same internal state [17–21]. The thermally average reaction rate is expressed as

$$\mathcal{K}(T) = \frac{2}{\sqrt{\pi}} T^{-3/2} \int_0^\infty E^{1/2} e^{-E/T} K dE. \quad (13)$$

III. APPLICATION TO THE EXPERIMENT

We take $V(r)$ to be the hard-core plus $-1/r^6$ potential. The effective potential is given by

$$V_{\text{eff}} = \begin{cases} \infty, & r < r_0, \\ -1/r^6 + V_{\text{sta}}(r), & r > r_0, \end{cases} \quad (14)$$

where r_0 is the position of the potential wall. The statistical potential $V_{\text{sta}}^{(2)}$ ($V_{\text{sta}}^{0(2)}$) for the case $N = 2$ is equivalent to the first-order quantum correction to the classical gas, namely the first-order approximation of the statistical potential V_{sta} (V_{sta}^0). We use formulas $V_{\text{sta}}^{(2)}$ and $V_{\text{sta}}^{0(2)}$ in the numerical calculation. For convenience, in the following, $V_{\text{sta}}^{(2)}$ and $V_{\text{sta}}^{0(2)}$ are

TABLE I. Fermi temperature T_{Fi} and \bar{r}_i (units of β_6) calculated according to the experimental data (the first two columns) [10].

Temperature T (nK) [10]	T/T_{Fi} [10]	Fermi temperature T_{Fi} (nK)	\bar{r}_i (units of β_6)
65	0.23	282.61	19.01
71	0.32	221.88	21.45
90	0.36	250.00	20.21
97	0.39	248.72	20.26
110	0.48	229.17	21.11
136	0.55	247.27	20.32
138	0.45	306.67	18.25
146	0.68	214.71	21.81
180	0.56	321.43	17.83
200	0.81	246.91	20.34
240	0.99	242.51	20.52
270	1.08	249.73	20.22
270	0.57	473.68	14.68
290	0.90	322.22	17.80
320	1.29	248.06	20.29
400	0.70	571.43	13.37
440	0.60	733.33	11.80

referred to as V_{sta} and V_{sta}^0 , respectively. The dispersion coefficient $C_6 = 17720$ a.u. [22] for the $^{40}\text{K}^{87}\text{Rb}$ molecule and the length scale $\beta_6 = 253.08$ a.u. [16]. The statistical potential V_{sta} exhibits a repulsive property in the Fermi gas and vanishes at high temperature, as shown in Fig. 1. In our calculation, the relative distance r in $V_{\text{sta}}(r)$ and $V_{\text{sta}}^0(r)$ is replaced by the average interparticle spacing \bar{r} , which is treated as an input parameter. The effect of the statistical potential on the scattering property is equivalent to that of a collision energy change. It is more unambiguous to write Eq. (1) as $[-d^2/dr^2 + L(L+1)/r^2 + V(r)]\psi(r) = [E - V_{\text{sta}}(\bar{r})]\psi(r)$. The volume is estimated to be $\mathcal{V} = N\bar{r}^3$.

Table I lists the Fermi temperature T_{Fi} and \bar{r}_i calculated according to the experimental data [10]. \bar{r}_i is obtained by using the relation $(3\pi^2)^{2/3}\hbar^2/(2m\bar{r}_i^2) = k_B T_{Fi}$ with $T \rightarrow 0$ [15]. In particular, $\bar{r} = 17.92\beta_6$ corresponds to the average Fermi temperature of the experimental data [10], $T_F = \sum_{i=1}^{17} T_{Fi}/17 = 318$ nK, according to the relation $(3\pi^2)^{2/3}\hbar^2/(2m\bar{r}^2) = k_B T_F$ with $T \rightarrow 0$ [15]. As shown by the blue solid line and red dashed line in Fig. 1, the smaller the distance \bar{r} , the stronger is the statistical potential V_{sta} . Squares and triangles represent the magnitudes of the statistical potential $V_{\text{sta}}(\bar{r}_i)$ for $T/T_F < 0.6$ and > 0.6 , respectively. For the points at 270 nK with $T/T_F < 0.6$ (square), 400 and 440 nK, their magnitudes are larger than those at low temperatures, and deviate from curves. This is caused by the small interparticle spacing, as shown in Table I.

In the spin-polarized Fermi gas of $^{40}\text{K}^{87}\text{Rb}$ molecules, the collisions are dominated by the p -wave scattering at ultralow temperature. The reaction rate is calculated by using Eq. (12). Figure 2 shows the thermally average reaction rates. The blue dotted-dashed and red solid lines show the calculated results with and without the statistical potential V_{sta} ,

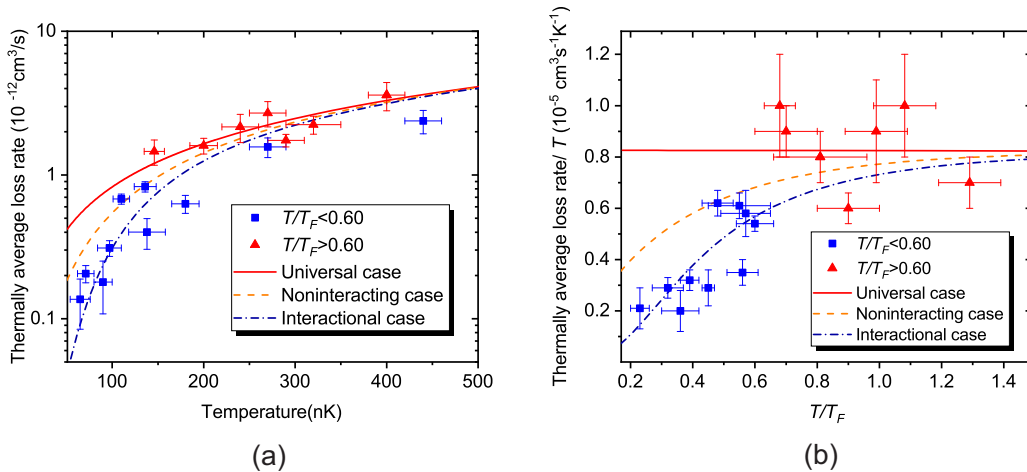


FIG. 2. (a) Thermally averaged reaction rates and (b) temperature-normalized reaction rates in theory (lines) and in experimental data (squares and triangles) [10]. Red solid lines show the calculated results without the statistical potential (universal case), orange dashed lines show the calculated results with the statistical potential V_{sta}^0 (noninteracting case, $\bar{r} = 17.92\beta_6$), and blue dotted-dashed lines show the calculated results with the statistical potential V_{sta} (interactional case, $\bar{r} = 17.92\beta_6$, $a_1 = -12.97a_0^3$). $T_F = 318$ nK.

respectively. The latter is a universal reaction rate. Our result for a universal reaction rate agrees well with the measured value in experiment for $T/T_F > 0.6$ (red triangles), and with a theoretical prediction by the capture dynamics model based on the statistical quantum mechanical approach [14]. The temperature-normalized reaction rate for $T/T_F > 0.6$ is a constant of $0.82 \times 10^{-5} \text{ cm}^3 \text{ s}^{-1} \text{ K}^{-1}$. The universal case obeys the Bethe-Wigner threshold law [10,11], indicating that the spatial correlation between particles has little effect on the reaction rate outside of the degenerate regime. The orange dashed lines show the results calculated by using V_{sta}^0 for an ideal gas. Though the interaction is not included, the suppression of the reaction rate has emerged, as shown in Fig. 2.

At ultralow temperature, the phase shift related to the p -wave scattering volume a_1 is given by

$$\tan \eta_{L=1}(k) = -k^3 a_1. \quad (15)$$

It is noted that the p -wave scattering volume a_1 is different from the complex scattering volume \tilde{a}_1 defined in Refs. [23,24]. The reaction rate scales with the inelastic part of the complex scattering volume \tilde{a}_1 in the universal case, and the relation between the complex scattering volume \tilde{a}_1 and the S matrix is given by $\tilde{a}_1 = (1 - S_{L=1})/[ik(1 + S_{L=1})]$ [23,24]. The p -wave scattering volume a_1 is treated as a fitting parameter. For a fixed a_1 , the phase shift $\eta_{L=1}(k)$ in Eq. (15) is substituted into Eq. (11) and an integration with respect to k is performed in order to obtain b_2 . When the interaction between particles is taken into account, the suppression of the reaction rate is well reproduced, as shown in the blue dotted-dashed line in Fig. 2, where a_1 is fitted to be $-12.97a_0^3$ with a_0 being the Bohr radius. With increasing temperature, the temperature-normalized reaction rate approximates a constant, $0.82 \times 10^{-5} \text{ cm}^3 \text{ s}^{-1} \text{ K}^{-1}$. Thus the degenerate case gradually evolves into the universal case. Furthermore, the magnitude of the statistical potential represents the strength of spatial correlation, and is calculated for all of the experimental data marked by red triangles ($T/T_F > 0.6$) and blue squares ($T/T_F < 0.6$), which are distributed around the blue solid line $\bar{r} = 17.92\beta_6$ in Fig. 1. Obviously, the correlated strengths between particles in the quantum degenerate regime (blue squares) are larger than those outside of the regime (red triangles). Therefore the reaction rates at $T/T_F < 0.6$ significantly deviate from those predicted by the threshold law.

The ratio of the reaction rate in the interaction case to the universal reaction rate is labeled as γ , which reflects the suppression of chemical reaction rate. For a fixed value of p -wave scattering volume ($a_1 = -12.97a_0^3$), Fig. 3 shows the ratios as a function of temperature when the average interparticle spacing \bar{r} is fixed at $20.00\beta_6$, $17.92\beta_6$, and $15.00\beta_6$. The suppression disappears when the ratio approaches unity. Because the density of the gas is proportional to $1/\bar{r}^3$, the suppression enlarges as the density increases. This is consistent with the experimental observation in which the chemical reaction is strongly suppressed in the center of the trap [10]. On the up axis of Fig. 3, the Fermi temperature T_F is taken to be 318 nK, which is the average value of the experimental data [10]. The black dotted line in Fig. 3 corresponds to the blue dotted-dashed line in Fig. 2. The increase of the magnitude

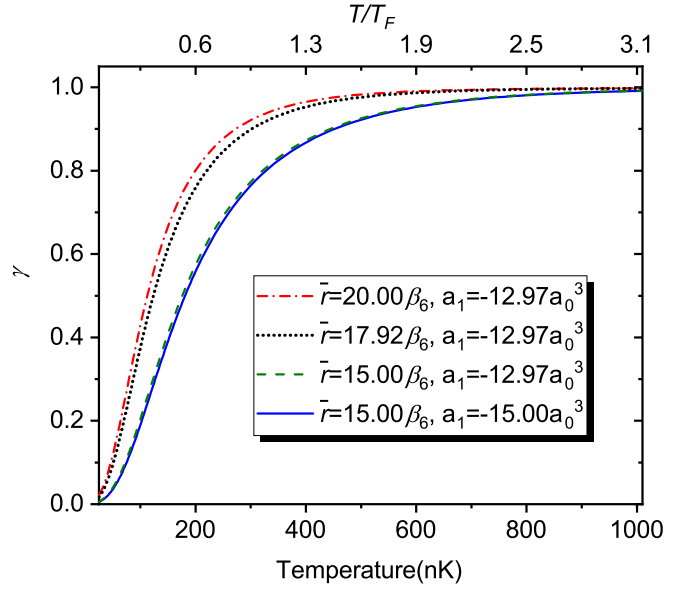


FIG. 3. The ratio γ as a function of temperature for the p -wave scattering volume $a_1 = -12.97a_0^3$ and $-15.00a_0^3$ and the average distance $\bar{r} = 20.00\beta_6$, $17.92\beta_6$, and $15.00\beta_6$. $T_F = 318$ nK.

of the p -wave scattering volume is also beneficial to the suppression, as shown in the blue solid and green dashed lines of Fig. 3. Though the calculation is performed for the $^{40}\text{K}^{87}\text{Rb}$ molecule, the results are also applicable to other Fermi molecular systems, where the variations are only mass m and coefficient C_6 . According to the relation $(3\pi^2)^{2/3}\hbar^2/(2m\bar{r}^2) = k_B T_F$ [15], the suppression for the heavy molecular system is stronger than that for the light one when T_F is fixed. In addition, the formation of a complex is an important factor [25–30]. The effect of the short-range interaction on the molecular collision was discussed in our previous work [17].

IV. CONCLUSION

In summary, we present a simple model used for exploring the suppressing reactivity in a degenerate Fermi gas. The influence of the interaction between particles is important in the degenerate regime. The formula of the statistical potential for a nonideal Fermi gas is derived. The suppression of the reaction rate is reproduced quantitatively by fitting the p -wave scattering volume to a specific value. From the magnitudes of the statistical potential, we can intuitively see that the spatial correlation strength in the quantum degenerate regime is larger than that outside the degenerate regime.

ACKNOWLEDGMENTS

We thank Jun Ye and Kyle Matsuda for providing the original experimental data. This work is supported by National Key R&D Program of China (No. 2018YFA0306503), National Natural Science Foundation of China (Grants No. 12104082 and No. 11274056), and Fundamental Research Funds for the Central Universities DUT19LK35.

- [1] M. H. Anderson, J. R. Ensher, M. R. Matthews, C. E. Wieman, and E. A. Cornell, *Science* **269**, 198 (1995).
- [2] C. C. Bradley, C. A. Sackett, J. J. Tollett, and R. G. Hulet, *Phys. Rev. Lett.* **75**, 1687 (1995).
- [3] K. B. Davis, M.-O. Mewes, M. R. Andrews, N. J. van Druten, D. S. Durfee, D. M. Kurn, and W. Ketterle, *Phys. Rev. Lett.* **75**, 3969 (1995).
- [4] B. DeMarco and D. S. Jin, *Science* **285**, 1703 (1999).
- [5] F. Schreck, L. Khaykovich, K. L. Corwin, G. Ferrari, T. Bourdel, J. Cubizolles, and C. Salomon, *Phys. Rev. Lett.* **87**, 080403 (2001).
- [6] A. G. Truscott, K. E. Strecker, W. I. McAlexander, G. B. Partridge, and R. G. Hulet, *Science* **291**, 2570 (2001).
- [7] I. Bloch, J. Dalibard, and W. Zwerger, *Rev. Mod. Phys.* **80**, 885 (2008).
- [8] S. Ospelkaus, K.-K. Ni, D. Wang, M. H. G. de Miranda, B. Neyenhuis, G. Quéméner, P. S. Julienne, J. L. Bohn, D. S. Jin, and J. Ye, *Science* **327**, 853 (2010).
- [9] S. A. Moses, J. P. Covey, M. T. Miecnikowski, B. Yan, B. Gadway, J. Ye, and D. S. Jin, *Science* **350**, 659 (2015).
- [10] L. De Marco, G. Valtolina, K. Matsuda, W. G. Tobias, J. P. Covey, and J. Ye, *Science* **363**, 853 (2019).
- [11] E. P. Wigner, *Phys. Rev.* **73**, 1002 (1948).
- [12] M. He, C. Lv, H.-Q. Lin, and Q. Zhou, *Sci. Adv.* **6**, eabd4699 (2020).
- [13] P. He, T. Bilitewski, C. H. Greene, and A. M. Rey, *Phys. Rev. A* **102**, 063322 (2020).
- [14] D. Yang, J. Huang, X. Hu, D. Xie, and H. Guo, *J. Chem. Phys.* **152**, 241103 (2020).
- [15] K. Huang, *Statistical Mechanics*, 2nd ed. (Wiley, New York, 1987).
- [16] B. Gao, *Phys. Rev. A* **78**, 012702 (2008).
- [17] Y. P. Bai, J. L. Li, G. R. Wang, Z. B. Chen, B. W. Si, and S. L. Cong, *Phys. Rev. A* **101**, 063605 (2020).
- [18] G. Quéméner and P. S. Julienne, *Chem. Rev.* **112**, 4949 (2012).
- [19] B. Gao, *Phys. Rev. Lett.* **105**, 263203 (2010).
- [20] G.-R. Wang, T. Xie, Y. Huang, W. Zhang, and S.-L. Cong, *Phys. Rev. A* **86**, 062704 (2012).
- [21] M. D. Frye, P. S. Julienne, and J. M. Hutson, *New J. Phys.* **17**, 045019 (2015).
- [22] P. S. Żuchowski, M. Kosicki, M. Kodrycka, and P. Soldán, *Phys. Rev. A* **87**, 022706 (2013).
- [23] Z. Idziaszek and P. S. Julienne, *Phys. Rev. Lett.* **104**, 113202 (2010).
- [24] K. Jachymski, M. Krych, P. S. Julienne, and Z. Idziaszek, *Phys. Rev. Lett.* **110**, 213202 (2013).
- [25] J. F. E. Croft, N. Balakrishnan, and B. K. Kendrick, *Phys. Rev. A* **96**, 062707 (2017).
- [26] X. Ye, M. Guo, M. L. Gonzalez-Martinez, G. Quéméner, and D. Wang, *Sci. Adv.* **4**, eaaq0083 (2018).
- [27] M.-G. Hu, Y. Liu, D. D. Grimes, Y.-W. Lin, A. H. Gheorghe, R. Vexiau, N. Bouloufa-Maafa, O. Dulieu, T. Rosenband, and K.-K. Ni, *Science* **366**, 1111 (2019).
- [28] A. Christianen, M. W. Zwierlein, G. C. Groenenboom, and T. Karman, *Phys. Rev. Lett.* **123**, 123402 (2019).
- [29] Y. Liu, M.-G. Hu, M. A. Nichols, D. D. Grimes, T. Karman, H. Guo, and K.-K. Ni, *Nat. Phys.* **16**, 1132 (2020).
- [30] J. F. E. Croft, J. L. Bohn, and G. Quéméner, *Phys. Rev. A* **102**, 033306 (2020).